

# Yeast Nucleolin Nsr1 Impedes Replication and Elevates Genome Instability at an Actively Transcribed Guanine-Rich G4 DNA-Forming Sequence

Shivani Singh,\* Alexandra Berroyer,\*\*† Minseon Kim,\*\*† and Nayun Kim\*.,†,1

\*Department of Microbiology and Molecular Genetics, University of Texas Health Science Center at Houston, Houston, Texas 77030 and †University of Texas (UT) Health MD Anderson Cancer Center Graduate School of Biomedical Sciences, Houston, Texas 77030

ORCID ID: 0000-0001-5299-0008 (M.K.)

**ABSTRACT** A significant increase in genome instability is associated with the conformational shift of a guanine-run-containing DNA strand into the four-stranded G-quadruplex (G4) DNA. The mechanism underlying the recombination and genome rearrangements following the formation of G4 DNA *in vivo* has been difficult to elucidate but has become better clarified by the identification and functional characterization of several key G4 DNA-binding proteins. Mammalian nucleolin (NCL) is a highly specific G4 DNA-binding protein with a well-defined role in the transcriptional regulation of genes with associated G4 DNA-forming sequence motifs at their promoters. The consequence of the *in vivo* interaction between G4 DNA and nucleolin in respect to the genome instability has not been previously investigated. We show here that the yeast nucleolin Nsr1 is enriched at a G4 DNA-forming sequence *in vivo* and is a major factor in inducing the genome instability associated with the cotranscriptionally formed G4 DNA in the yeast genome. We also show that Nsr1 results in impeding replication past such a G4 DNA-forming sequence. The G4-associated genome instability and the G4 DNA-binding *in vivo* require the arginine-glycine-glycine (RGG) repeats located at the C-terminus of the Nsr1 protein. Nsr1 with the deletion of RGG domain supports normal cell growth and is sufficient for its pre-rRNA processing function. However, the truncation of the RGG domain of Nsr1 significantly weakens its interaction with G4 DNA *in vivo* and restores unhindered replication, overall resulting in a sharp reduction in the genome instability associated with a guanine-rich G4 DNA-forming sequence. Our data suggest that the interaction between Nsr1 with the intact RGG repeats and G4 DNA impairs genome stability by precluding the access of G4-resolving proteins and impeding replication.

**KEYWORDS** G4 DNA; genome instability; nucleolin; replication

**G**-QUADRUPLEXES or G4 DNAs are unique noncanonical four-stranded DNA structures that can form from guanine-rich nucleic acid sequences (Bochman *et al.* 2012; Maizels and Gray 2013). Four guanine molecules interact via Hoogsteen bonds to yield G-quartets that in turn stack

on top of each other, held together by intervening loops of variable length and sequence to form the G4 DNA. The size and orientation of the loops can determine the relative stability of various G4 DNA configurations (Kim 2019). Though some computational analyses revealed that >375,000 and >1,400 G4 motifs are in the human and the *Saccharomyces cerevisiae* genomes, respectively, it is still unclear how many of these sequences with high quadruplex-forming potential actually assume the stable G4 configuration *in vivo* (Huppert and Balasubramanian 2005; Capra *et al.* 2010). Nevertheless, it is becoming quite evident that these structural transformations potentially provide a substantial informational capacity to DNA with specific functions (Maizels and Gray 2013). Recent bioinformatic studies in human, yeast, and bacterial genomes have revealed that G4 motifs are not randomly

Copyright © 2020 Singh *et al.*

doi: <https://doi.org/10.1534/genetics.120.303736>

Manuscript received September 28, 2020; accepted for publication October 21, 2020; published Early Online October 26, 2020.

Available freely online through the author-supported open access option.

This is an open-access article distributed under the terms of the Creative Commons Attribution 4.0 International License (<http://creativecommons.org/licenses/by/4.0/>), which permits unrestricted use, distribution, and reproduction in any medium, provided the original work is properly cited.

Supplemental material available at figshare: <https://doi.org/10.25386/genetics.13135823>.

<sup>1</sup>Corresponding author: 6431 Fannin St. MSE R262, Houston, TX, 77030. E-mail: [nayun.kim@uth.tmc.edu](mailto:nayun.kim@uth.tmc.edu)

located within genomes but are particularly enriched in certain functional regions, such as those in ribosomal and telomeric DNA, G-rich micro- and minisatellites, and mitotic and meiotic double-strand break (DSB) sites (Todd *et al.* 2005; Rawal *et al.* 2006; Eddy and Maizels 2008). Their high prevalence in and around genes particularly proximal to transcriptional start sites suggests a possible role as *cis*-acting regulatory elements (Du *et al.* 2008; Hershman *et al.* 2008; Moruno-Manchon *et al.* 2017).

The presence of G4 DNA was recently shown to impair DNA replication by hindering the progress of replicative polymerases, and the failure to resolve these structures transforms the sequence motifs into potential hotspots for genomic instability (Sarkies *et al.* 2010). In humans, the occurrence of G4 DNA motifs reportedly overlap with recombination-prone regions such as certain proto-oncogenes and the sites of frequent translocation breakpoints (Siddiqui-Jain *et al.* 2002; Seenisamy *et al.* 2004). Consistently, chromosomal translocations in the proximity of G4 motifs have been observed in leukemias and lymphomas (Bacolla *et al.* 2016). The potential to adopt G4 DNA has additionally been correlated with a number of human neurological diseases, such as frontotemporal dementia (FTD), amyotrophic lateral sclerosis, Alzheimer's and fragile X syndrome (Majounie *et al.* 2012; Haeusler *et al.* 2014; Maizels 2015). The resolution of G4 DNA structures is thus imperative in preserving genome integrity.

The genetic tractability of *S. cerevisiae* has provided considerable insight into the mechanisms involved in maintaining stability of G-rich repetitive sequences. The instability at the G-rich human minisatellite CEB1 inserted in the *S. cerevisiae* genome was shown to be dependent on the ability of the CEB1 motif to form G4 DNA and was not observed with other tandem repeats lacking G4 DNA-forming potential (Lopes *et al.* 2011; Piazza *et al.* 2012). The G4-forming sequence derived from the guanine-run containing immunoglobulin switch Mu ( $S_{\mu}$ ) region becomes highly unstable when actively transcribed in the context of the yeast genome. Transcription conferred a critical strand bias, since genome rearrangements at  $S_{\mu}$  were elevated only when the guanine-runs were located on the nontranscribed strand (Kim and Jinks-Robertson 2011). The direction of replication and transcription, when in a head-on orientation, further elevated genome instability at the  $S_{\mu}$  sequence (Yadav *et al.* 2014). At the  $S_{\mu}$  sequence, the lack of functional topoisomerase 1 (Top1) significantly elevated various types of genome instability, likely by facilitating the structural transition of a G-rich sequence to a G4 structure due to the accumulation of negative helical stress in DNA. The loss of heterozygosity and copy number alterations (deletions and duplications), both of which are frequently observed in cancer genomes, were also elevated when the  $S_{\mu}$  sequence was actively transcribed.

The biological functions of G4 DNA are largely dependent on the protein factors that modulate the G4-conformation and/or serve as a bridge to recruit additional protein

regulators (Brázda *et al.* 2014). These G4-binding proteins can be classified into three functional groups: (1) telomere-related proteins, such as the shelterin complex, human CST (CTC1-STN1-TEN1), and yeast Rap1 and Est1 (Pedroso *et al.* 2009; Li *et al.* 2013; Bhattacharjee *et al.* 2017); (2) proteins that unfold and/or process the G4 structure, such as the helicases including RecQ family helicases hBLM, hWRN, ySgs1, and yPif1 (Mendoza *et al.* 2016); and (3) proteins that stabilize G4 structures including MAZ and nucleophosmin (Gallo *et al.* 2012; Cogoi *et al.* 2014). Mutations in some of these G4-interacting proteins have been linked to genetic diseases such as Werner syndrome, Fanconi anemia, and cancer (Cantor *et al.* 2001; Seal *et al.* 2006; Wu *et al.* 2008; Mendoza *et al.* 2016). A defective BLM helicase failed to unwind G4 DNA and caused increasing recombination frequencies and a high incidence of cancer in Bloom's syndrome (Sun *et al.* 1998). More recently, the cotranscriptional activator Sub1, which interacts with both G4 DNA and the G4-helicase Pif1, was shown to suppress the G4-associated genome instability by facilitating the recruitment of Pif1 helicase to cotranscriptionally formed G4 DNA structures (Lopez *et al.* 2017).

The human nucleolin (NCL) is a highly abundant and conserved nucleolar phosphoprotein. Its major function is in ribosomal RNA maturation with additional roles in chromatin remodeling, transcription, and apoptosis (Tajrishi *et al.* 2011). The altered expression and subcellular localization of NCL is a common biomarker of a variety of cancers demonstrating its clinical relevance (Otake *et al.* 2007; Berger *et al.* 2015; Satake *et al.* 2018; Kim 2019). Although initially described as a G4 RNA-binding protein, more recent evidence indicates that NCL preferentially and selectively binds both endogenous and exogenous G-rich sequences that can fold into G4 DNA (Dempsey *et al.* 1999; Hanakahi *et al.* 1999; Fry 2007). It is suggested that NCL acts as a chaperone to promote the correct folding of complex nucleic acid structures (González *et al.* 2009; González and Hurley 2010; Tosoni *et al.* 2015). Together with the nuclear riboprotein hnRNPd, NCL forms a lymphocyte-specific complex LR1 (lipopolysaccharide responsive factor 1), which binds at the G4 DNA-forming Immunoglobulin heavy chain (IgH) switch regions (Dempsey *et al.* 1999). The binding of NCL to the G4-forming hexanucleotide repeat expansion (HRE) (GGGGCC)<sub>n</sub> in C9orf72 has been reported to be responsible for the initiation of molecular cascades that lead to neurodegenerative diseases (Haeusler *et al.* 2014). NCL is composed of three main structural domains; the amino-terminal domain containing four acidic stretches was shown to induce chromatin decondensation through interaction with histone 1H (Erard *et al.* 1988), while the central region containing tandem RNA-binding domains (RBDs) and the multiple RGG (arginine/glycine/glycine) boxes at the C-terminal domain contribute to its high-affinity interaction with G4 DNA (Hanakahi *et al.* 1999; Ghosh and Singh 2018).

Similar to the human protein, the yeast nucleolin Nsr1 has been demonstrated to be involved in pre-rRNA processing and

ribosome production (Kondo and Inouye 1992; Lee *et al.* 1992). While there are no significant sequence similarities in the amino-terminal regions between yNsr1 and hNCL, the C-terminal half of yNsr1, consisting of two tandemly repeated putative RBDs and the multiple RGG (arginine/glycine/glycine) motifs, has a high sequence similarity to the carboxyl-terminal part of hNCL (37% identity in 249 amino acids) (Lee *et al.* 1991; Kondo and Inouye 1992). Unlike the plethora of studies highlighting the NCL/G4 interaction, the role of yeast Nsr1 related to G4 DNA has not been extensively studied. In the current study, we examined whether the yeast Nsr1 has a role in the genome instability associated with G4-forming sequences. We identified an important biological role of Nsr1 in enhancing various types of genome rearrangements associated with cotranscriptionally formed G4 DNA. We show that the yeast Nsr1 is enriched at the highly transcribed G4 DNA-forming motif *in vivo* and that the disruption of Nsr1 lowers the G4-associated recombination, while its overexpression further exacerbates instability in a dose-dependent manner in cells lacking Top1. The C-terminal RGG domain of Nsr1 is required to form a complex with G4 DNA *in vivo*, to obstruct replication, and to promote genetic instability, but is dispensable for the rRNA processing function of Nsr1. Our results point to an important role of Nsr1 in G4-associated genome maintenance.

## Materials and Methods

### Yeast strains and plasmids

Yeast strains used for the mutation and recombination assays were derived from YPH45 (*MATa, ura3-52 ade2-101 trp1Δ1*). Construction of strains containing the *pTET-lys2-GTOP* or *-GBTM* constructs were previously described (Kim and Jinks-Robertson 2011). Gene deletions were carried out via the one-step allele replacement by amplification of loxP-flanked marker cassettes. Nsr1-expression plasmid was constructed by amplifying NSR1 ORF along with 490 nt upstream and 250 nt downstream from the yeast genomic DNA and cloning into the yeast *CEN* vector pRS316. The deletion constructs N-Term Nsr1 and C-term Nsr1 have been previously described (Azevedo *et al.* 2015). The expression plasmid for human nucleolin was constructed by amplifying the NCL ORF from GFP-nucleolin (#28176; Addgene) using primers NCL-For and NCL-1XHA Rev (Supplemental Material, Table S1). The BamHI/XhoI-digested NCL PCR product was cloned into BamHI/XhoI-digested pGPD2 (#43972; Addgene). The NCL-ΔRGG plasmid was similarly created using primers NCL-For and NCLΔRGG -1XHA Rev (Table S1).

### Determination of rates

Recombination rates and 95% confidence intervals were determined using the method of the median as described previously (Spell and Jinks-Robertson 2004). Twelve to 36 individual cultures were used to determine each rate and the associated 95% confidence intervals. Recombination

rates are considered to be statistically different when the 95% confidence intervals, which are indicated in each graph as error bars, do not overlap. For the gross chromosomal rearrangement (GCR) assay, 5-ml cultures in YPD medium (1% yeast extract, 2% Bacto-peptone, 2% dextrose, and 250 μg/ml adenine hemisulfate) were inoculated with single colonies and grown for 3 days at 30°. Cells were then plated either on YPD-agar or synthetic complete dextrose medium lacking arginine (SCD-arg) and containing canavanine (60 mg/liter) and 5-fluoroorotic acid (5-FOA; 1 g/liter) (Chen and Kolodner 1999).

### Growth curve

Growth curve and doubling time measurement: eight independent cultures of each genotype were grown to midlogarithmic phase, diluted to  $\sim 1 \times 10^6$  cells/ml and incubated in a 96-well plate at 30°. OD<sub>600</sub> was measured automatically every 10 min. Doubling time was calculated using the following equation: Doubling time = [hours cells grown Ln(2)]/[Ln (Nt/N0)], where Nt and N0 are the OD<sub>600</sub> at two different times in log phase of growth.

### Northern blot analysis

Northern blot analysis of the ribosomal RNAs was carried out as previously described (Han and van Hoof 2016).

### Chromatin immunoprecipitation

For Chromatin IP (ChIP), a previously described protocol was used (Lopez *et al.* 2017) with the following modifications. Anti-FLAG antibody-conjugated beads (Cat# A8592; Sigma), were used in pull-down. Ct values for each ChIP samples were first normalized to the corresponding input samples, and then divided by the values for the *CAN1* locus to calculate the relative fold enrichment. Primers used in the qPCR analysis were previously described (Lopez *et al.* 2017). *P*-values were calculated using the Student *t*-test. For the TMPyP4 ChIP, the cells were grown at 30° in liquid YPD containing 50 μM TmPyP4. Next day, they were diluted in liquid YPD containing 50 μM TmPyP4 and grown till mid-log phase (O.D<sub>600</sub> 0.7–0.8). Cells were cross-linked and further processed as above.

### Cell synchronization and time course experiment

Cell synchronization and sample collection was carried out as described with slight modifications (Owiti *et al.* 2018). Briefly, 30° grown, log phase cells (OD<sub>600</sub> ~0.5–0.6) with *bar1Δ* were arrested in late G1 phase using 50 ng/ml α-factor peptide (Sigma) for ~120 min, released by washing with fresh YPD medium with 50 μg/ml Pronase (Sigma), and then allowed to proceed through a synchronous cell cycle at 21°. Samples were removed at 10-min intervals and immediately treated with buffer containing 0.1% sodium azide.

### DNA extraction and ddPCR

Yeast genomic DNA extraction from the cells collected at 10-min intervals after the release from α-factor was carried

out as described (Batrakou *et al.* 2018). DNA concentration was measured using the Qubit double-stranded DNA (dsDNA) HS assay (ThermoFisher). The DNA was sonicated for two cycles of 15 sec ON/90 sec OFF in Bioruptor (Diagenode) at 4°. The ddPCR reaction consisted of 1.5–2 ng of sonicated genomic DNA, 1× QX200 ddPCR EvaGreen Supermix (Bio-Rad) and primers (200 nM final each). The samples were processed using the QX200 Droplet Digital PCR system and analyzed with the QuantaSoft software (Bio-Rad). The primers are listed in Table S1. For calculating the copy number, each time point values of the “ARS306,” “KanMX,” and “STE50” loci were normalized to time 0 value of the “ARS306” locus, and for the “KanMX” and “STE50” loci, they were further normalized to the “KanMX” (time 0) and “STE50” (time 0), respectively. Data from at least three independent experiments were used to calculate the standard deviation. *P*-values were calculated using Student *t*-test (Graphpad Prism).

### Data availability

The authors state that all data necessary for confirming the conclusions presented in the manuscript are represented fully within the manuscript. Supplemental material available at figshare: <https://doi.org/10.25386/genetics.13135823>.

## Results

### *Nsr1* enhances G4-mediated recombination in cells lacking topoisomerase 1

To understand the elevated genome instability associated with G4-forming sequences, we previously developed a recombination reporter assay in the yeast model system (Kim and Jinks-Robertson 2011). In this reporter assay, a model G4-forming sequence from the murine immunoglobulin heavy chain switch Mu region ( $S_{\mu}$ ) (Figure S1A) was inserted into the yeast genome within the *LYS2* gene under the control of a tetracycline/doxycycline-repressible promoter (*pTET*). The  $S_{\mu}$  sequence was inserted either in the physiological (GTOP) or into the inverted orientation (GBTM), placing the G-runs in the nontranscribed strand (NTS) or in the transcribed strand (TS), respectively (Figure S1B). The formation of G4 DNA is favored when the G-rich strand located on the NTS is transformed into a single-stranded state during transcription, freeing the guanine bases to interact with each other through Hoogsteen base-pairing. When G-runs are located in the TS, they will be occupied in base-pairing with the nascent RNA strand and will not be free to fold into G4 DNA. Thus, any factors involved in the formation or stability of G4 DNA should affect the recombination occurring at the *pTET-lys2-GTOP* construct, with little to no effect on the rate of recombination at the *pTET-lys2-GBTM* construct (Kim and Jinks-Robertson 2011; Yadav *et al.* 2014; Lopez *et al.* 2017).

To determine whether *Nsr1* plays a role in the G4-mediated genome instability, we deleted the *NSR1* gene in strains

containing the *pTET-lys2-GTOP* or -GBTM construct and checked the rate of recombination at this locus. In the wild-type (WT) background, the deletion of *NSR1* resulted in a slow-growth phenotype of the cells as previously reported (Lee *et al.* 1992). Under high transcription conditions, the rates of recombination at the *pTET-lys2-GTOP* or -GBTM cassette in *nsr1Δ* strains were not changed from those in WT strains (Figure 1A).

Topoisomerase I (Top1) was previously identified to be a crucial factor for G4-mediated genome instability in yeast (Kim and Jinks-Robertson 2011; Yadav *et al.* 2014; Yadav *et al.* 2016). Accumulation of negative supercoils in *top1Δ* yeast cells was shown to promote recombination at the *pTET-lys2-GTOP* construct. To determine whether *Nsr1* modulates the G4-associated genomic instability in the absence of Top1, we deleted the *NSR1* gene in a *top1Δ* background. The rate of recombination for the *pTET-lys2-GTOP* was reduced by ~threefold in the *top1Δ nsr1Δ* strain compared to *top1Δ* (Figure 1B). For the *pTET-lys2-GBTM*, the rates of recombination were indistinguishable between *top1Δ* and *top1Δ nsr1Δ* backgrounds. When the transcription from the *pTET* promoter was repressed by the addition of 2 μg/ml doxycycline in the media, the deletion of *NSR1* did not affect the rates of recombination in WT and reduced slightly in a *top1Δ* background (Figure S2).

The catalytically inactive mutant of Top1 (Top1-Y727F) with the mutation of catalytic tyrosine to phenylalanine results in complete ablation of its function in removal of supercoils, while not affecting its DNA-binding activity (Megenigal *et al.* 1997). Possibly due to its high G4-binding ability, the expression of Top1-Y727F results in recombination rates that are ~eightfold higher than in the absence of Top1 (*top1Δ*) (Yadav *et al.* 2016). When *Nsr1* was disrupted in the *top1Y727F* backgrounds, the recombination rate at the *pTET-lys2-GTOP* cassette was significantly decreased and was comparable to the rate in the *top1Δ* strain (Figure 1C). The disruption of *Nsr1* did not affect the rate of recombination at the *pTET-lys2-GBTM* cassette.

### *Nsr1* does not affect the G4-associated recombination in RNase H-deficient cells

Disrupting both RNase H1 and RNase H2 in yeast leads to the accumulation of transcription-associated RNA:DNA hybrids or R-loops (Wahba *et al.* 2011) and subsequently elevates levels of recombination for both the *pTET-lys2-GTOP* and -GBTM constructs (Kim and Jinks-Robertson 2011). The G-loop, a higher order structure consisting of R-loop and G4 DNA, could arise from either the enhanced negative supercoils leading to G4 formation upon disruption of Top1 or due to the failure to degrade RNA leading to R-loops upon disruption of RNase Hs. We have previously shown that the elevated recombination rates for the *pTET-lys2-GTOP* and -GBTM constructs in *rnh1Δ rnh201Δ* backgrounds are reduced by either repressing transcription from *pTET* (Kim and Jinks-Robertson 2011) or by removing the RNA:DNA hybrids by ectopic expression of RNase H1 (Yadav *et al.*

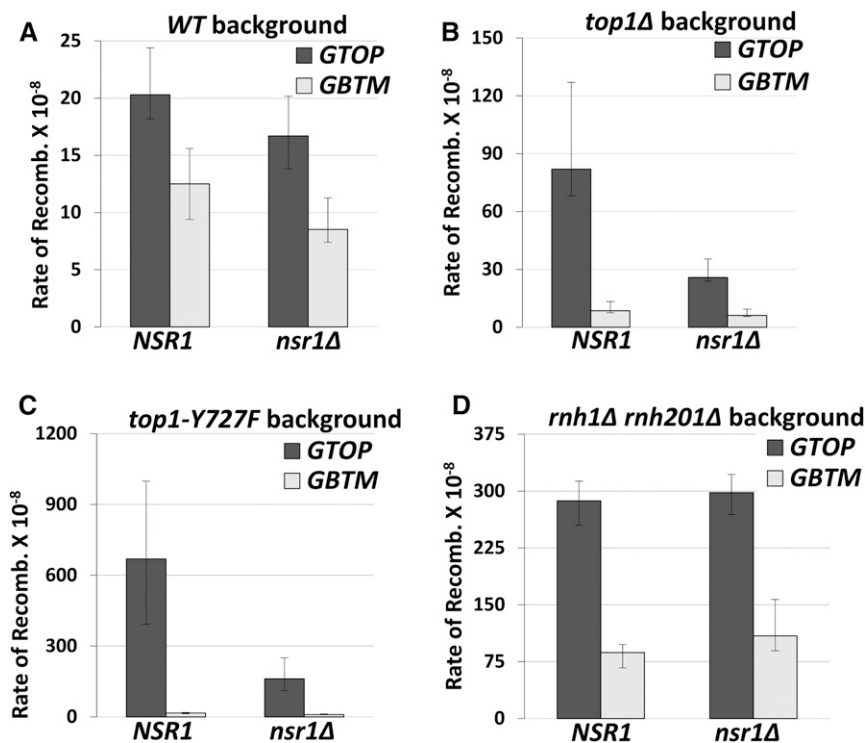


**Figure 1** The rates of G4-associated recombination in *nsr1Δ* strains. Guanine-runs are on the nontranscribed, top strand in a single-stranded state in *pTET-lys2-GTOP* cassette and on the transcribed strand annealed to the nascent RNA in the *pTET-lys2-GBTM* cassette. All graphs show the rates of recombination ( $\times 10^{-8}$ ). Error bars indicate 95% confidence intervals. Two rates are considered statistically different when the confidence intervals do not overlap. The rates, numbers of cultures used in fluctuation analyses, and 95% confidence intervals are listed in Table S2. (A) Recombination rates in WT backgrounds. (B) Recombination rates in *top1Δ* backgrounds. (C) Recombination rates in *top1Y727F* backgrounds. (D) Recombination rates in *rnh1Δ rnh201Δ* backgrounds.

2016). Therefore, we checked whether, in addition to reducing recombination rates in a *top1Δ* strain, the deletion of Nsr1 could affect the R-loop-mediated enhanced recombination rates. In the triple deletion mutant *rnh1Δ rnh201Δ nsr1Δ*, there was no significant alteration in the rate of recombination for the *pTET-lys2-GTOP* or *-GBTM* construct (Figure 1D). This data suggests that Nsr1-induced genomic instability is specific to G4 DNA formed due to the enhanced negative helical torsion under high transcription in a *top1Δ* background and not due to the RNA: DNA hybrid accumulation.

#### ***Nsr1* promotes GCRs in the *top1Δ* backgrounds**

We previously reported that, in the absence of functional Top1, the cotranscriptionally formed G4 DNA at the *pTET-lys2-GTOP* construct leads to the increase in ectopic recombination as well as in the GCRs (Yadav *et al.* 2014). To measure the rates of GCR, we used a modified form of the GCR reporter system developed by Chen and Kolodner (1999). In this reporter system, the *URA3* gene was integrated into the left arm of chromosome V (CHR5) replacing the *HXT13* gene located ~8.5 kb centromere-distal to the *CAN1* gene. The *pTET-lys2-GTOP* or *-GBTM* cassette containing the  $S_{\mu}$  G4 motif, as described before (Yadav *et al.* 2014), is integrated immediately centromere-proximal to *CAN1*. The loss of functional *CAN1* or *URA3* results in resistance to the drug canavanine (Can) or 5-fluoroorotic acid (5-FOA), respectively. Thus, by simultaneous selection against two counterselectable markers (*URA3* and *CAN1*), complex genome rearrangement can be measured. Using this modified GCR assay, it was previously shown that in the high transcription conditions,

the disruption of Top1 leads to a significantly higher (~30-fold) GCR rate for *pTET-lys2-GTOP*, where guanine-runs are present on the NTS, compared to the *pTET-lys2-GBTM* construct where guanine-runs are on the TS (Yadav *et al.* 2014). When we deleted *NSR1* in WT backgrounds, there was no change in the GCR rates for *pTET-lys2-GTOP* or *-GBTM* (Figure 2A). However, the disruption of Nsr1 in *top1Δ* backgrounds resulted in a significant, ~sixfold reduction of the GCR rates for the *pTET-lys2-GTOP* but not for the *-GBTM* construct (Figure 2B). To test whether the function of Nsr1 is specific to the  $S_{\mu}$  G4-mediated genome instability or extends to other G4 motifs as well, we used a GCR reporter modified to contain the G4 motif from the TCF3 translocation breakpoint (Williams *et al.* 2015). In a similar manner to the GCR reporter containing  $S_{\mu}$  G4, when Nsr1 was disrupted in a *top1Δ* strain but not in a WT strain, the GCR rates were severely lowered by ~ninefold at the *pTET-lys2-GTOP* (*TCF3*) construct, while at the *pTET-lys2-GBTM* (*TCF3*) construct the GCR rates were not significantly changed (Figure 2, C and D).

#### ***The RGG domain of Nsr1 is necessary for the elevated G4-associated recombination but not for the support of normal cell growth or pre-rRNA processing***

We considered the possibility that the effect of *NSR1* deletion on the rate of recombination could be attributed to the marked slow-growth phenotype reported for *nsr1Δ* cells (Kondo and Inouye 1992; Lee *et al.* 1992). We measured cell growth and calculated doubling time in WT, *top1Δ*, *nsr1Δ*, and *top1Δ nsr1Δ* strains. While the doubling time of a WT (~96 min) and *top1Δ* strain (~99 min) was comparable, the

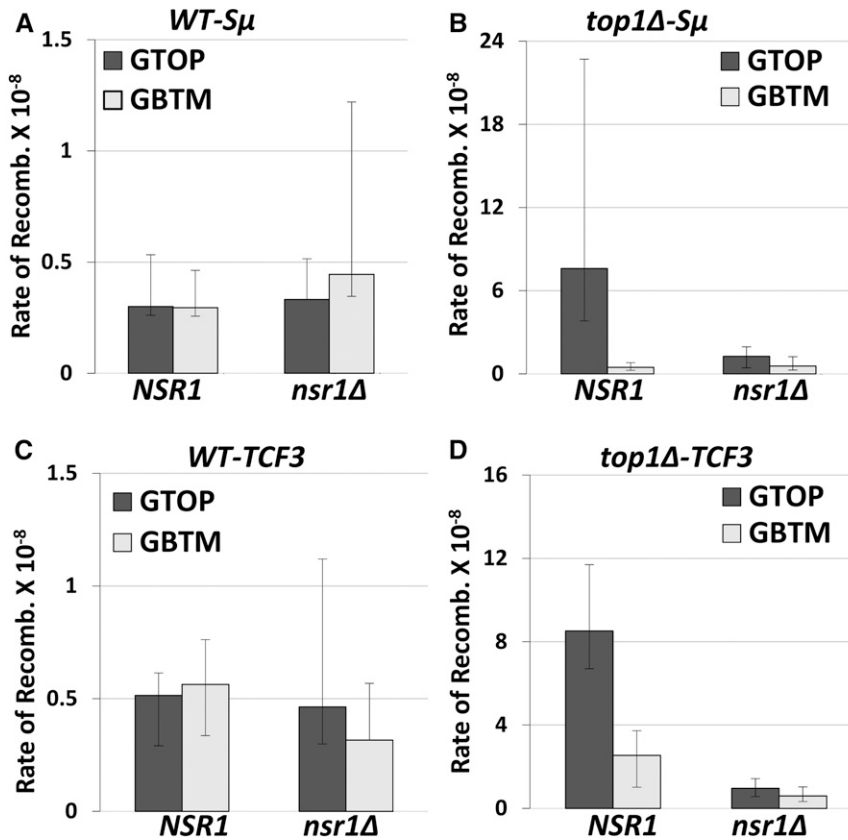


**Figure 2** Rates of gross chromosomal rearrangement (GCR) in *nsr1Δ* strains. All graphs show the rates of 5-FOA<sup>r</sup>/CAN<sup>r</sup> or GCRs ( $\times 10^{-8}$ ). The rates of GCRs occurring at CHR5 containing the *pTET-lys2-GTOP* or *-GBTM* cassette are determined by the method of median. 95% Confidence intervals are indicated by the error bars. Two rates are considered statistically different when the confidence intervals do not overlap. GCR rates, numbers of cultures used in fluctuation analyses, and the 95% confidence intervals are listed in Table S4. GCR rates in strains with the reporter cassette containing the  $S_{\mu}$ -G4 in (A) WT backgrounds and (B) *top1Δ* backgrounds. GCR rates in strains with the reporter cassette containing TCF3-G4 in (C) WT backgrounds and (D) *top1Δ* backgrounds.

*nsr1Δ* mutant strain showed a significantly longer doubling time of 141 min (Figure S3A). This growth defect was slightly further aggravated upon the deletion of the *TOP1* gene; the doubling time was  $\sim$ 152 min for the *top1Δ nsr1Δ* mutants. Nsr1 has been reported to be involved in pre-rRNA processing in yeast, and deletion of the *NSR1* gene leads to defective 35S pre-rRNA processing; 35S accumulates and 20S is greatly reduced (Lee *et al.* 1992). We carried out Northern hybridization analysis using oligonucleotide probes that were designed to hybridize to pre-rRNA and confirmed the sharp decrease in the 20S and the concomitant accumulation of unprocessed 35S in our *nsr1Δ* strain (Figure S3, B and C). The deletion of the *TOP1* gene had no or little effect on the pre-rRNA processing in WT or *nsr1Δ* backgrounds, respectively. The C-terminal RGG domain of nucleolin has been shown to be important for inducing and stably binding G4 structures (González and Hurley 2010; Ghosh and Singh 2018). To test whether the deletion of the RGG domain results in a cell growth defect similar to the complete null allele, we replaced the WT *NSR1* allele with the *nsr1ΔRGG* allele at its endogenous chromosomal location on the left arm of chromosome 7 in a *top1Δ* background. In this mutant strain (*top1Δ nsr1ΔRGG*), a growth defect was not observed, and the doubling time was similar to the WT or *top1Δ* strain rather than *nsr1Δ* or *top1Δ nsr1Δ*. The pre-rRNA processing efficiency in the *top1Δ nsr1ΔRGG* strain was also similar to that of the WT or *top1Δ* strain with a similar ratio of 20S/35S.

We also observed no differences in 7S pre-rRNA level within the different mutants (Figure S3B). Thus, the RGG domain appears dispensable for the normal cell growth and pre-rRNA processing function.

To further test whether Nsr1 or Nsr1ΔRGG can elevate the recombination rate at the *pTET-lys2-GTOP*, a full-length *NSR1* gene and the N-terminal 1–350 residues of Nsr1 lacking the RGG domain (*nsr1ΔRGG*) along with its own promoter (*pNSR1*) were each cloned into the centromeric plasmid pRS316 (Figure 3A). The ectopic expression of full-length Nsr1 in the *top1Δ nsr1Δ* double mutant strain elevated the rate of recombination for the *pTET-lys2-GTOP* by 8.5-fold, thereby resulting in the rates of recombination that were similar to a *top1Δ* transformed with the empty vector (Figure 3B). However, the expression of Nsr1ΔRGG did not elevate the rate of recombination at the *pTET-lys2-GTOP* cassette. The rates of recombination of the *pTET-lys2-GBTM* cassette were not affected by either Nsr1-or Nsr1ΔRGG expression. This result, which indicates that the RGG domain is necessary to elevate recombination at the *pTET-lys2-GTOP* cassette, was confirmed using the yeast strains where the WT *NSR1* allele was replaced with the *nsr1ΔRGG* allele at its endogenous chromosomal location on the left arm of chromosome 7. Similar to the results obtained with plasmid-expressed Nsr1ΔRGG, the deletion of the RGG domain (*nsr1ΔRGG*) at its genomic location resulted in the reduced recombination rate at the *pTET-lys2-GTOP* cassette similar to the complete

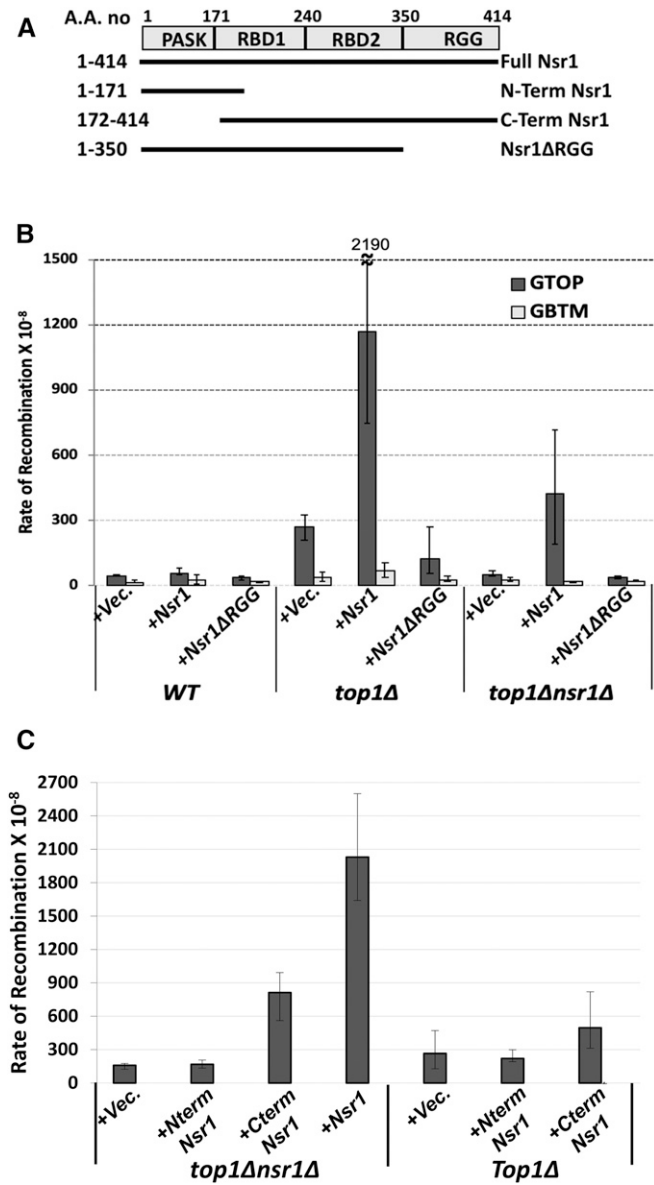


**Figure 3** Complementation of NSR1-deletion. (A) Domain organization of Nsr1. The deletion constructs used for complementation are indicated. (B and C) Graphs show the rates of recombination ( $\times 10^{-8}$ ). Error bars indicate 95% confidence intervals. Two rates are considered statistically different when the confidence intervals do not overlap. For B, indicated yeast strains are transformed with a *CEN* plasmid [an empty vector (Vec.) or a plasmid with either pNSR1-Nsr1 or pNSR1-Nsr1ΔRGG construct]. The rates, numbers of cultures used in fluctuation analyses, and 95% confidence intervals are listed in Table S5. For C, indicated yeast strains are transformed with a  $2\mu$  plasmid [an empty vector (Vec.) or a plasmid with either pADH1-Nsr1, pADH1-Nterm Nsr1, or pADH1-Cterm Nsr1 construct]. The rates, numbers of cultures used in fluctuation analyses, and 95% confidence intervals are listed in Table S6.

deletion (*nsr1Δ*) (Figure S3D). Together, these results indicate that even though Nsr1ΔRGG was sufficient to support normal yeast cell growth and rRNA processing functions (Figure S3, A–C), it is necessary for elevated genome instability at the G4-forming *pTET-lys2-GTOP* cassette.

We next expressed the N-terminal (1–171aa; N-term Nsr1 in Figure 3A) or the C-terminal region (C-Term; 172–414aa) of Nsr1 using  $2\mu$  plasmid constructs with the highly expressed *ADH1* promoter. The N-term construct was unable to complement for the loss of Nsr1 in enhancing G4-induced recombination (Figure 3C). However, the C-terminal deletion construct significantly elevated the rates of recombination albeit not as robustly as the full-length Nsr1. The rates of recombination for the C-terminal deletion construct were 5.1-fold higher than the rates of recombination for the empty vector. Although the effect of the C-terminal construct ( $2\mu$  plasmid with *ADH1* promoter) cannot be directly compared to the effect of Nsr1ΔRGG (*CEN* plasmid with *NSR1* promoter), these results overall suggest that the RBD and RGG domains at the C-terminal of Nsr1 are required for promoting G4-associated instability.

When we expressed the full-length Nsr1 and Nsr1ΔRGG in WT strains with the normal endogenous level of Nsr1, there was no effect of overexpression of the full-length Nsr1 constructs, while the Nsr1ΔRGG construct reduced the rates of recombination slightly (Figure 3B). In the *top1Δ* strain, the overexpression of full-length Nsr1 elevated the rates of recombination at the *pTET-lys2-GTOP* cassette by  $\sim 4.5$ -fold compared to vector alone. When the Nsr1ΔRGG construct was expressed in the *top1Δ* strain, the rates of recombination were consistently lower than the empty vector. The N-term Nsr1 (1–171) was unable to induce recombination and showed rates of recombination that were similar to the empty vector. The C-terminal Nsr1 (172–414) expression resulted in about twofold higher recombination rates (Figure 3C). These results suggest that Nsr1 increases recombination in a dose-dependent manner, and this function requires the RGG domain.

We also tested whether the highly conserved human NCL can complement the loss of Nsr1 in yeast. When NCL was expressed from a plasmid (*CEN*, *pNSR1*), the rate of recombination at the *pTET-lys2-GTOP* cassette was elevated by  $\sim$ twofold (Figure 4). And like the yeast Nsr1ΔRGG, the human NCLΔRGG with C-terminal deletion failed to increase the rate of recombination in *top1Δ nsr1Δ* cells. In *top1Δ* cells, the expression of NCL, but not NCLΔRGG, resulted in a further twofold increase in recombination at the *pTET-lys2-GTOP*, indicating that the function of Nsr1 with an intact RGG domain in mediating the G4-associated genome instability is conserved in the human homolog (Figure 4).

#### Nsr1 binds to the G4 DNA *in vivo*

To determine whether Nsr1 interacts with G4 structures *in vivo*, we measured the association of Nsr1 and G4 DNA by using a chromatin immuno-precipitation (ChIP) assay. ChIP was performed in WT, *top1Δ*, and *top1Δ nsr1ΔRGG* cells containing either the *pTET-lys2-GTOP* or-GBTM construct and expressing Nsr1 or Nsr1ΔRGG with a C-terminal 3XFlag tag. Following the pull-down with  $\alpha$ Flag antibody-conjugated beads, qPCR analysis was done to determine the enrichment of Nsr1 at a locus 100 bp from the G4 insertion site (“G4 insert”)



and a locus ~3 kb away from the G4 insertion site (“3 kb”). We observed ~twofold enrichment of Nsr1 at the G4 locus when the G4 sequence was in the *GTOP* orientation, but not in the *GBTM* orientation in a *top1Δ* background ( $P < 0.0001$ ) (Figure 5, A and B). Further, the enrichment of Nsr1 was significantly higher at the switch region G4 sequence insertion site than the 3' region of the *lys2* sequence 3 kb away ( $P = 0.0021$ ) (Figure 5A). Nsr1ΔRGG, which is missing the C-terminal RGG domain, however, was not significantly enriched at the G4 locus in *top1Δ* cells ( $P = 0.0009$  compared to full-length Nsr1). For the mammalian NCL, *in vitro* interaction with G4 DNA is significantly enhanced by its C-terminal domain (Hanakahi *et al.* 1999; Hanakahi *et al.* 2000; González and Hurley 2010; Tosoni *et al.* 2015). Similarly, Nsr1 forms a complex with a G4-forming oligonucleotide *in vitro*, and such interaction is diminished either by the mutation of guanine-runs involved in the quadruplex formation or by the deletion of C-terminal RGG repeats of Nsr1 protein (Figure S4). These data indicate that Nsr1 specifically associates with the G4 DNA accumulated under high transcription conditions and that this association between G4 and Nsr1 requires the C-terminal RGG repeats.

When we repeated the ChIP experiments in yeast cells treated with G4 stabilizing ligand TMPyP4 prior to cross-linking, enrichment of Nsr1 at the G4 locus when the G4 sequence was in the *GTOP* orientation was elevated by ~threefold with no change in the enrichment at the non-G4 locus 3 kb away (Figure 5C). However, enrichment of Nsr1 was also elevated at the G4 locus when the G4 sequence was in the *GBTM* orientation (Figure 5D), possibly indicating that the guanine-runs present on the TS in the *GBTM* orientation can be induced to form relatively stable G4 DNA structure by TMPyP4.

#### ***Nsr1*-disruption allows for better access by activation-induced deaminase to the single-stranded DNA in the G4-prone sequence**

Formation of a stable Nsr1–G4 DNA complex could elevate genome instability at the *pTET-lys2-GTOP* by precluding the access of G4-resolving proteins such as DNA helicases to G4 DNA. To test whether the presence of Nsr1 impedes the accessibility of protein factors to G4 DNA, we expressed human Activation-induced deaminase (hAID) in the yeast strains containing the *pTET-lys2-GTOP* or *-GBTM* construct. hAID converts cytosine to uracil and is required for the somatic hyper-mutation (SHM) of immunoglobulin variable region genes as well as the heavy chain class switch recombination (Peled *et al.* 2008). We previously showed that the ectopic expression of hAID in the WT and *top1Δ* yeast cells resulted in a higher rate of recombination at the *pTET-lys2-GBTM* than *-GTOP* in both strain backgrounds (Kim and Jinks-Robertson 2011). This difference was partly attributed to the larger number of cytosines present on the single-stranded NTS in the *GBTM* orientation compared to the *GTOP* orientation (358 vs. 117 cytosines), since hAID specifically targets the cytosines located on the single-stranded DNA.

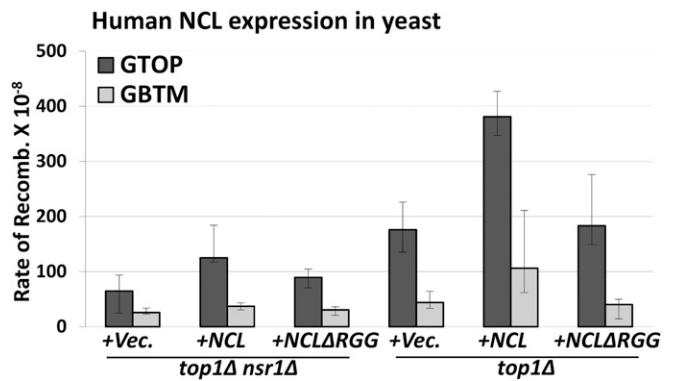


**Figure 4** Overexpression of Nsr1 or hNCL. The *top1Δ nsr1Δ* or *top1Δ* yeast cells were transformed with empty vector (+Vec), hNCL-expression plasmid (+NCL) and hNCL-ΔRGG followed by fluctuation analysis to determine the rates of recombination. All graphs show the rates of recombination ( $\times 10^{-8}$ ). Error bars indicate 95% confidence intervals. Two rates are considered statistically different when the confidence intervals do not overlap. The rates, numbers of cultures used in fluctuation analyses, and 95% confidence intervals are listed in Table S7.

We postulated that the NSR1–G4 DNA complex could further impede the accessibility of hAID to those cytosines on the NTS in the *pTET-lys2-GTOP* construct located proximal to the G4 structure. Thus, we tested whether the cytosines present on the NTS in the *GTOP* orientation could become more accessible to hAID in the absence of Nsr1 protein. When we expressed hAID, the rate of recombination at the *pTET-lys2-GBTM* cassette was elevated by about four- to fivefold in the WT, *top1Δ*, and *top1Δ nsr1Δ* strains. For the *pTET-lys2-GTOP* construct, the rate of recombination was not changed by the expression of hAID in WT and *top1Δ* strains, but increased by about threefold in a *top1Δ nsr1Δ* strain (Table 1). This increased rate of recombination could reflect less-restricted access of hAID to the cytosines in the absence of a G4 DNA–Nsr1 complex on the NTS.

#### ***Nsr1* obstructs replication at a G4 DNA-containing locus**

The above genetic data and enrichment of Nsr1 at the G4-insert loci led us to hypothesize that Nsr1 binds to G4 DNA *in vivo* and obstructs replication. To determine whether the Nsr1–G4 DNA complex functions as a replication block, we measured the DNA copy number of specific genomic loci throughout S phase. Droplet digital PCR (ddPCR), which provides an absolute quantification of the target DNA with high precision, accuracy, and sensitivity (Pinheiro *et al.* 2012), was used to determine the replication kinetics as inferred from the copy number changes throughout the S phase (see Materials and Methods). Our approach was modified from a previously reported use of ddPCR in determining replication timing of multiple sites in the yeast and human genomes (Batrakou *et al.* 2018). To determine the locus-specific replication timing, cells were first arrested with  $\alpha$ -factor and released into S phase. Flow cytometry confirmed synchronous progression through S phase upon release from  $\alpha$ -factor (Figure S5). DNA samples collected every 10 min



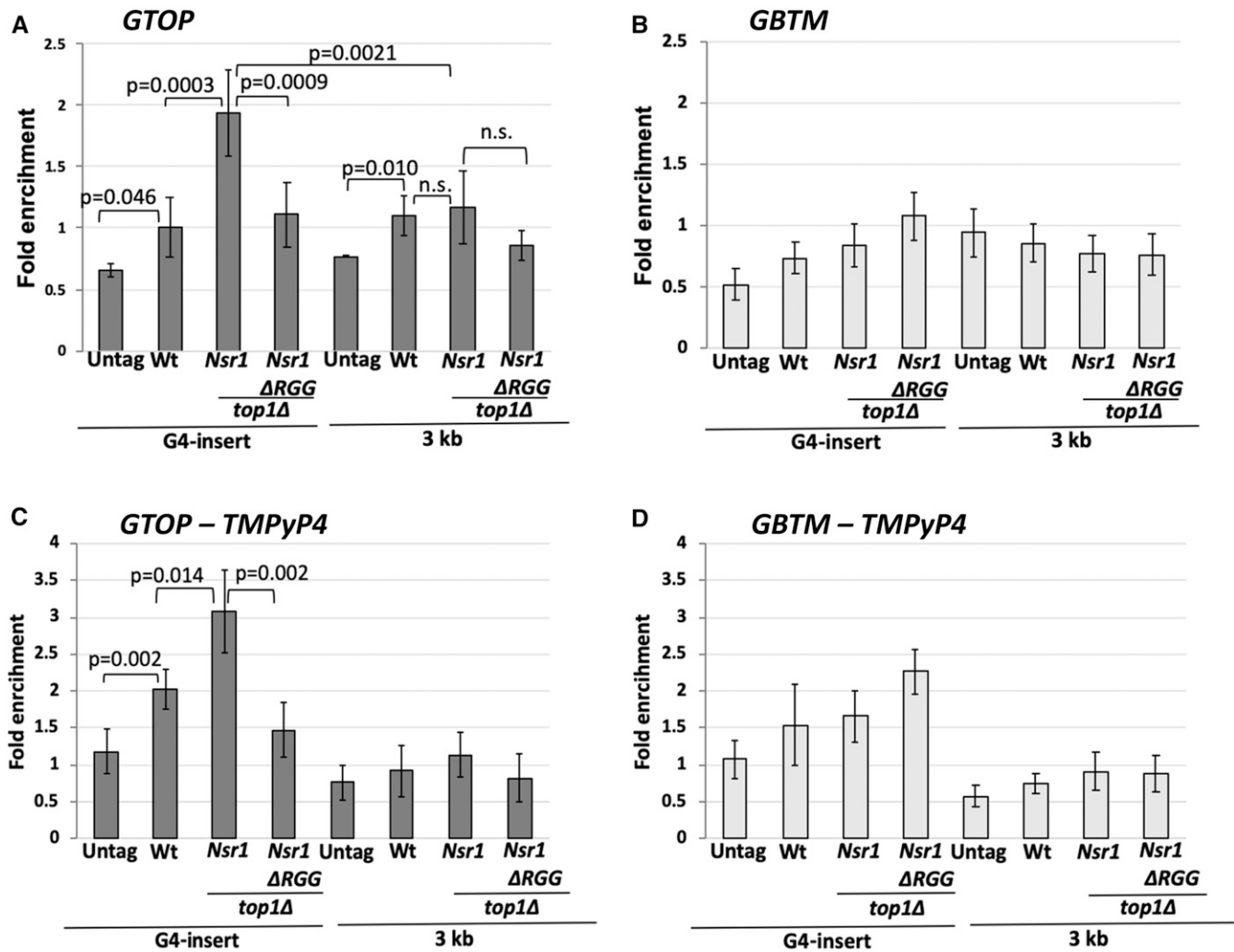


**Figure 5** Nsr1 binding to G4 DNA *in vivo* requires the RGG domain. ChIP was carried out with an  $\alpha$ Flag antibody and chromatin fractions prepared from yeast cells with indicated genetic backgrounds. 5 $\zeta$ BGL and STP primers were previously described and anneal within the *LYS2* ORF at  $\sim$ 100 and  $\sim$ 3000 bp from the *S $\mu$*  sequence insertion site, respectively. All values are based on at least six independent samples with the exception of the no-tag samples ( $N = 3$ ) and the standard deviations are indicated by error bars. *P*-values shown were calculated using Student's *t*-test. (A) GTOP strains; (B) GBTM strains; (C) GTOP strains treated with TMPyP4; (D) GBTM strains treated with TMPyP4.

from 0 to 100 min after the release were used to determine the copy numbers at three different loci; “ARS306” – near the early firing autonomously replicating sequence on chromosome III, “KanMX” – between “ARS306” ( $\sim$ 8 kb distal) and the *pTET-lys2-GTOP* cassette ( $\sim$ 2 kb distal), and “STE50” – further distal from “ARS306” ( $\sim$ 14 kb distal) compared to the *pTET-lys2-GTOP* cassette ( $\sim$ 4 kb distal) (Figure 6A). The other nearest origin of replication is *ARS305*, which is located  $>$ 23 kb from the “STE50” locus. As marked by the blue arrows in Figure 6A, replication in this genomic region was previously determined to predominantly originate from *ARS306* and proceed past “KanMX”, *pTET-lys2-GTOP*, and then “STE50” loci (Kim *et al.* 2007). Replication kinetics at these three genomic loci in yeast cells in a *top1 $\Delta$*  background with either an *NSR1* or *nsr1 $\Delta$ RGG* allele were compared; the significant growth defect in *nsr1 $\Delta$*  cells compared to *NSR1* cells, which is not present in cells with the *nsr1 $\Delta$ RGG* allele

(Figure S3A), would have interfered with a straightforward comparison. In respect to the recombination occurring at the *pTET-lys2-GTOP* cassette, the *nsr1 $\Delta$ RGG* allele is indistinguishable from the *nsr1 $\Delta$*  null allele (Figure 3B and Figure S3D).

During the S phase, the copy number at each genomic locus is expected to progressively increase from one to two as replication proceeds. The time at which replication completes and the copy number reaches two will be mostly dependent on proximity to the relevant replication origin, *ARS306*. In *top1 $\Delta$  nsr1 $\Delta$ RGG* cells containing the *pTET-lys2-GTOP* cassette, the copy number of “ARS306” locus reached two at around 50–60 min after the release from  $\alpha$ -factor (Figure 6B). A similar pattern for this locus was observed in *top1 $\Delta$*  cells, which express full-length Nsr1 protein. For the *top1 $\Delta$*  and *top1 $\Delta$  nsr1 $\Delta$ RGG* strains containing the *pTET-lys2-GBTM* cassette, the copy number of “ARS306” locus also reached two at

**Table 1 Effect of hAID expression on G4-associated recombination rates**

Genotype		Recombination rate $\times 10^{-8}$ (C.I. <sup>a</sup> )		Fold change: hAID/vector
		Empty vector	hAID	
pTET-lys2-GTOP	WT	20.4 (15.1–27.9)	31.7 (16.2–60.2)	1.5
	<i>top1Δ</i>	220 (177–322)	219 (137–661)	0.99
	<i>top1Δnsr1Δ</i>	20.6 (13.7–27.8)	54.1 (46.3–65.8)	2.6
pTET-lys2-GBTM	WT	12.7 (8.0–17.1)	59.1 (44.7–84.5)	4.6
	<i>top1Δ</i>	11.4 (8.92–15.3)	45.6 (38.8–51.4)	4.0
	<i>top1Δnsr1Δ</i>	10.4 (8.3–15.5)	56.7 (29.7–150)	5.4

<sup>a</sup> 95% confidence interval.

around 50–60 min after the release from  $\alpha$ -factor with no significant difference between the two strain backgrounds (Figure S6A). For the “KanMX” locus in the strains with the *pTET-lys2-GBTM* cassette, the time after release from  $\alpha$ -factor required to reach the copy number of two was between 60 and 70 min regardless of the strain background (Figure S6B). Also, in the *top1Δ* cells with the *pTET-lys2-GTOP* cassette, there was only a slight but statistically nonsignificant lag in replication at the “KanMX” locus compared to the *top1 nsr1ΔRGG* cells (Figure 6C). At the “STE50” locus, there was a more significant difference in replication kinetics between the *top1Δ nsr1ΔRGG* and *top1Δ* strains (Figure 6D). While the copy number of this locus reached two around 70 min after the release from  $\alpha$ -factor in *top1 nsr1ΔRGG* cells, in *top1Δ* cells the copy number of “STE50” was significantly below two at the 70-min time point, reaching two only 80 to ~90 min after  $\alpha$ -factor release.

For *top1Δ* and *top1Δ nsr1ΔRGG* strains containing the *pTET-lys2-GBTM* cassette, no difference in the replication kinetics was observed with the copy number at “STE50” reaching two around 70 min after  $\alpha$ -factor release (Figure S6C). The *pTET-lys2-GBTM* cassette contains the identical guanine-run-containing sequence from the mouse  $S_{\mu}$  region as the *pTET-lys2-GTOP* cassette but in reverse orientation in respect to the direction of transcription within the context of the *LYS2* gene (Kim and Jinks-Robertson 2011). We have previously shown that there is no significant difference in the transcription rates of these two cassettes (Yadav *et al.* 2014). During transcription, the DNA strand containing guanine-runs is the NTS in the *pTET-lys2-GTOP* cassette and TS in the *pTET-lys2-GBTM* cassette. Although identical in sequence content, the strand difference conferred by transcription allows higher potential for the guanine-run-containing strand to assume G4 DNA due to its transient single-strandedness in the context of the *pTET-lys2-GTOP* cassette. When the replication kinetics were compared between strains containing either the *pTET-lys2-GTOP* or *pTET-lys2-GBTM* cassette, a significant difference was noted at the STE50 locus, which is replicated after the G4 DNA-forming *pTET-lys2-GTOP* or *-GBTM* cassette, only when full-length Nsr1 was present (Figure 7). Nsr1 or *Nsr1ΔRGG* did not affect the replication kinetics at “ARS306,” which is replicated prior to the *pTET-lys2-GTOP* or *-GBTM* cassette.

## Discussion

Although initially described as a sequence-specific RNA-binding protein, human NCL preferentially binds to G-quadruplex structures over RNA substrates and plays a crucial role in G4 metabolism (González *et al.* 2009; González and Hurley 2010; Haeusler *et al.* 2014). In this study, we have explored the possibility that the yeast homolog Nsr1 also contributes to G4 DNA metabolism. We showed that, similar to the human homolog, yeast Nsr1 is significantly enriched *in vivo* at a G4 reporter construct (Figure 5). Such enrichment was only observed when the guanines are on the top, NTS of an actively transcribed gene (*i.e.*, *pTET-lys2-GTOP*) in a *top1Δ* background, which is the condition with the significant elevation of G4-associated recombination. Nsr1-enrichment is significantly reduced ~3 kb away from the G4 motif sequence even though it is within the same transcribed unit, which further supports the specificity of Nsr1 interaction with G4 DNA.

The disruption of Nsr1 substantially decreases the G4-associated genomic instability as manifested by the decreased rates of recombination and of GCR in a *top1Δ* background by about three- and sixfold, respectively (Figures 1 and 2). The reduction in genome instability in the absence of Nsr1 was not specific to the switch region G-rich sequence, as GCRs occurring at a different G-rich motif from the human TCF3 gene were also reduced upon deletion of *NSR1* (Figure 2D). Additionally, overexpression of Nsr1 led to further elevation of recombination specifically at the *pTET-lys2-GTOP* cassette in a *top1Δ* background (Figure 3B). One interpretation of these surprising results is that the consequence of the association between Nsr1 and G4 DNA is the elevated genome instability. Both  $S_{\mu}$ G and TCF3 fragments used in our reporter assays are typical of the recently characterized Long G4-capable regions (LG4s) that contain a series of neighboring G4-capable sequences (Williams *et al.* 2020). The function of potential multiple, closely spaced G4 DNA associated with LG4s has only been recently studied. It is therefore possible that Nsr1-dependent elevation of genome instability is limited to such LG4s rather than a singly present G4 motif.

Genome instability associated with G4-structures should be prevented by the activity of G4-unwinding DNA helicases including yeast Sgs1 and Pif1 (Huber *et al.* 2002; Paeschke *et al.* 2013). We considered the possibility that Nsr1 can occlude DNA helicases from recognizing and then resolving G4

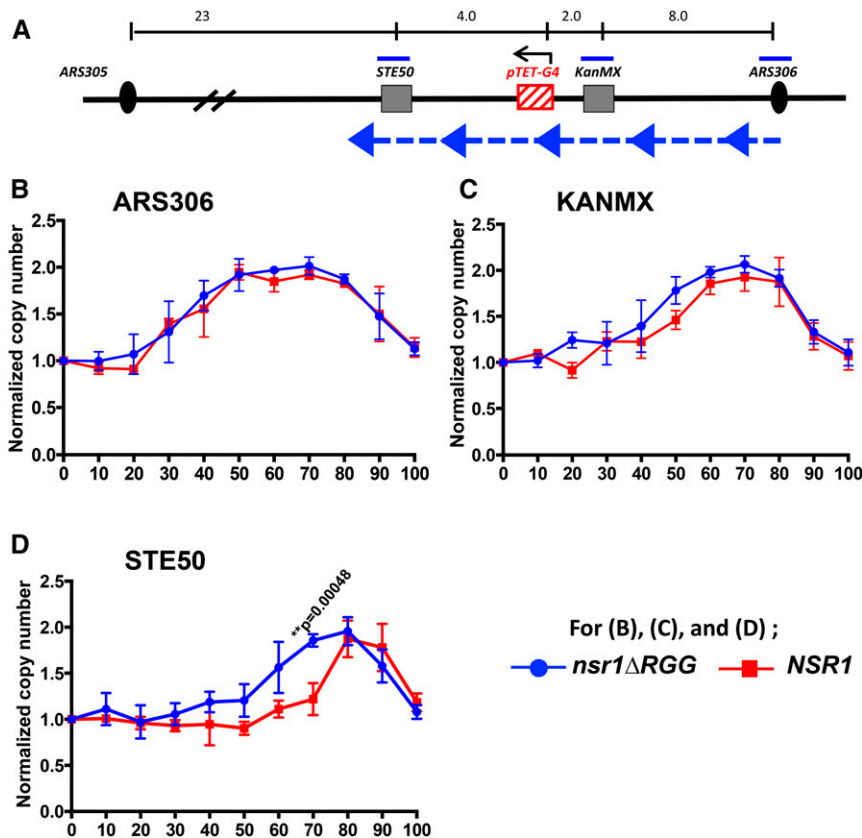


**Figure 6** DNA replication timings and copy number changes determined by ddPCR. (A) A schematic drawing of the regions proximal to the *pTET-lys2-GTOP* cassette on yeast chromosome III. The locations of primers used in ddPCR are indicated by blue bars. The black arrow over pTET-G4 indicates the direction of transcription. Large blue arrow heads with dashed blue line indicate the direction of replication fork movement. For the sequences of the primers, see Table S1. The distance indicated above in kilobases are estimates and not to scale. (B–D) For *top1*Δ and *top1*Δ *nsr1*ΔRGG strains, DNA samples analyzed by ddPCR were extracted at the indicated time points (minutes after the release from α-factor). For calculating the copy number, each time point value of “ARS306,” “KanMX,” and “STE50” loci was normalized to time 0 value of the “ARS306” locus. And for “KanMX” and “STE50” loci, they were further normalized to the “KanMX” at time 0 and “STE50” at time 0, respectively. Data from at least three independent experiments was used to calculate mean and standard deviations (indicated by error bars). *P*-values were calculated using Student’s *t*-test. All *P*-values < 0.005 are indicated. Normalized copy number of (B) “ARS306”, (C) “KanMX”, and (D) “STE50” loci.

DNA. Human nucleolin NCL, in fact, was reported to prevent Werner helicase from unwinding G4 oligos *in vitro* (Indig *et al.* 2012). When we expressed hAID to induce cytosine deamination and subsequent recombination, those cytosines present on the NTS at the G4 DNA-forming *pTET-lys2-GTOP* cassette were more susceptible to hAID processing in a *top1*Δ *nsr1*Δ background than in a *top1*Δ background (Table 1), supporting the idea that the regions proximal to the G4 DNA are in a less accessible conformation in the presence of Nsr1. These results show that Nsr1–G4 DNA complexes are capable of precluding access of DNA-interacting protein factors such as hAID to G4 DNA. We speculate that if the access of G4-specific helicase were to be precluded in a similar manner, the failure to resolve G4 DNA is expected to result in elevated genome instability.

Located C-terminal to the multiple RBDs, yeast Nsr1 and human NCL contain six and nine repeats of arginine-glycine-glycine or RGG motifs, respectively, which are found in proteins associated with important nucleic acid-mediated functions such as transcription, pre-mRNA splicing, DNA damage signaling, and mRNA translation (Thandapani *et al.* 2013). Other proteins with verified roles in DNA metabolism and cancer development that contain RGG motifs include Mre11 (a DSB-processing enzyme), Mll4 (a histone methyltransferase), and Ews (Ewings sarcoma protein; DNA damage response protein). Recently, the RGG-box of hnRNPA1, a member of ribonucleoproteins, was shown to

bind specifically to the telomeric G4 DNA (Ghosh and Singh 2018). In yeast Nsr1, RGG motifs also appear to play an important function. Yeast cells expressing Nsr1 with the truncation of this motif (*Nsr1*ΔRGG) do not show the severe defects in the pre-rRNA processing and cell growth that are typical of the *nsr1*Δ cells (Figure S3, A–C). However, when we deleted the RGG domain from Nsr1, the resulting *Nsr1*ΔRGG construct lost the ability to complement the full-length Nsr1 in promoting genome instability at the *pTET-lys2-GTOP* cassette either in a *top1*Δ *nsr1*Δ or *top1*Δ background (Figure 3B). This could be due to weaker interaction between G4 DNA and the *Nsr1*ΔRGG mutant protein. Earlier biochemical analysis showed that the RGG domain of hNCL is required for high-affinity interaction with G4-forming oligos *in vitro* (Hanakahi *et al.* 1999). Our ChIP results, showing that *in vivo* binding of Nsr1 to a G4 DNA-containing genomic locus is dependent on the presence of the RGG domain as well as the results of *in vitro* pull-down assay showing that binding to G4-forming oligo is significantly reduced when the RGG domain is absent, further support this hypothesis (Figure 5 and Figure S4).

Overall, our data indicate that the elevation of G4-associated genomic instability by Nsr1 requires a strong physical interaction with G4 DNA as mediated by the RGG domain. Such a conclusion suggests that Nsr1 binding leads to stabilization of the cotranscriptionally formed G4 DNA and that the Nsr1-bound G4 DNA forms a nucleoprotein complex that can

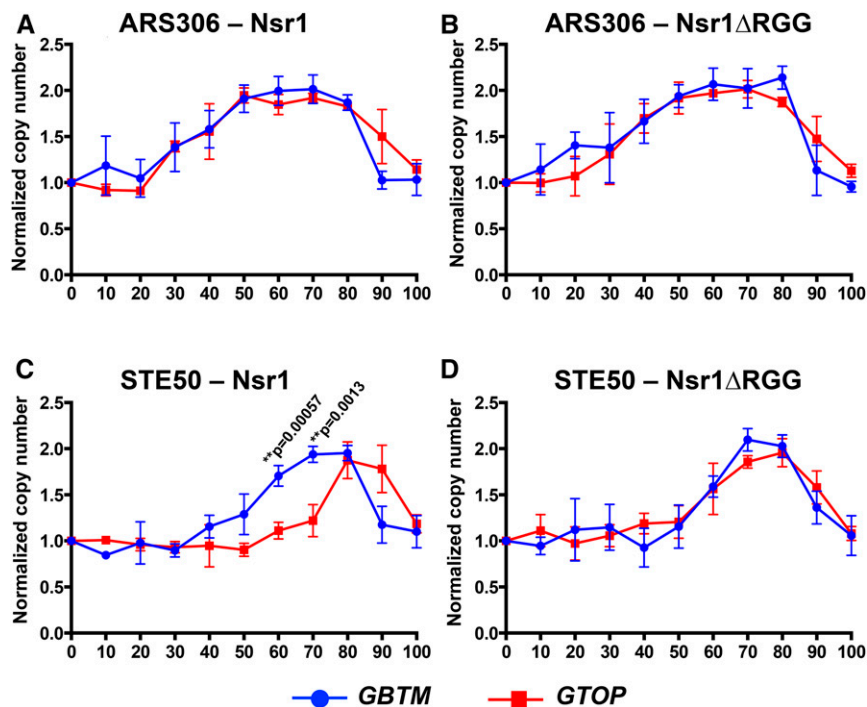


**Figure 7** DNA replication timings near *pTET-lys2-GTOP* vs. *pTET-lys2-GBTM*. The DNA copy numbers determined from 0 to 100 min after the release from  $\alpha$ -factor were plotted. The data used for the graphs are identical to those shown in Figure 6 and Figure S6. (A) “ARS306” in *top1Δ* background, (B) “ARS306” in *top1Δ nsr1ΔRGG* background, (C) “STE50” in *top1Δ* background, and (D) “STE50” in *top1Δ nsr1ΔRGG* background.

significantly impede replication. Nonhistone protein–DNA complexes forming a replication block have been previously reported for the origin of replication (ORC) complex and Rap1 (Ivessa *et al.* 2003). To determine whether the Nsr1–G4 DNA complex poses a physical replication obstruction, we measured the replication kinetics of genomic region proximal to the G4 DNA-containing *pTET-lys2-GTOP* cassette using the ddPCR approach, where the copy number of the specific genomic loci was tracked through a single synchronized S phase. As shown in Figure 6, replication proceeds from ARS306 through “KanMX” regions and the *pTET-lys2-GTOP* cassette before it passes the “STE50” locus. As would be expected from the replication block forming at the *pTET-lys2-GTOP*, no significant deviation in replication kinetics was observed at the sites located between the replication origin and the *pTET-lys2-GTOP* (i.e., “ARS306” and “KanMX”; Figure 6, B and C). However, the replication fork must proceed past the G4-containing *pTET-lys2-GTOP* region before it reaches “STE50”, where the significant delay in replication was observed in the presence of Nsr1 in a *top1Δ* background (Figure 6D). This delay in replication progress, just as the elevated G4-associated recombination, required the RGG domain of Nsr1; replication at “STE50” proceeded with significantly faster kinetics in cells expressing Nsr1ΔRGG compared to cells expressing the full-length Nsr1. This difference between Nsr1ΔRGG and Nsr1 further supports the idea that the strong physical interaction between Nsr1 and G4 DNA underlies both G4-specific replication obstruction and genome instability. Replication obstruction incurred by the combination of Nsr1 and G4 DNA is more clearly illustrated when the replication kinetics in cells containing cassette is

compared to those in cells containing the non-G4-forming *pTET-lys2-GBTM* cassette as shown in Figure 7. A very significant delay in the replication progress is observed at the “STE50” locus downstream of the G4 reporter only in cells expressing full-length Nsr1. In *nsr1ΔRGG* backgrounds, the replication kinetics at this locus showed no significant differences between the strains containing either the *pTET-lys2-GTOP* or -*GBTM* construct.

In summary, we have identified a novel function of yeast Nsr1 as a G4 DNA-binding protein. We first demonstrate here that Nsr1 is specifically enriched at a cotranscriptionally formed G4 DNA *in vivo* and that Nsr1-interaction with G4 DNA results in a significant replication impediment in a G4 DNA-specific manner. This key finding suggests that the formation of a stable Nsr1–G4 DNA complex functioning as a replication obstruction underlies the significant elevation in G4-associated genome instability. Importantly, data presented here point to the requirement of the conserved RGG domain at the C-terminal end of Nsr1 in promoting instability at G4 DNA. This result calls for further study into the conformational changes associated with the RGG domain in the Nsr1–G4 DNA complex that could enable such a complex to function as a replication obstacle.

### Summary

Here, we report a novel finding that the conserved G4 DNA-binding protein Nsr1 elevates recombination and chromosomal rearrangement occurring at a G4 DNA-forming sequence in the yeast genome. Elevated instability requires the C-terminally located RGG domain of Nsr1. Connection between genome instability and the function of Nsr1 to form a

stable complex with G4 DNA led to the hypothesis that the Nsr1–G4 DNA complexes impede replication. We demonstrate that the presence of Nsr1 in fact slows replication past a G4 DNA-containing site and that the RGG domain is required to facilitate such a replication impediment.

## Acknowledgments

The authors thank A. Saiardi of University College London, UK for the gift of plasmids with the C-term and N-term Nsr1 constructs. We also thank the members of the Kim laboratory for discussion and critical reading of the manuscript. The authors declare that there are no conflicts of interest. N.K. was supported by grants from the National Institutes of Health (R01 GM116007) and Welch Foundation (AU1875). A.B. was supported by grant R01 GM116007-S1. M.K. was supported by grant R01GM099790 to Ambro van Hoof.

## Literature Cited

- Azevedo, C., T. Livermore, and A. Saiardi, 2015 Protein polyphosphorylation of lysine residues by inorganic polyphosphate. *Mol. Cell* 58: 71–82. <https://doi.org/10.1016/j.molcel.2015.02.010>
- Bacolla, A., J. A. Tainer, K. M. Vasquez, and D. N. Cooper, 2016 Translocation and deletion breakpoints in cancer genomes are associated with potential non-B DNA-forming sequences. *Nucleic Acids Res.* 44: 5673–5688. <https://doi.org/10.1093/nar/gkw261>
- Batrakou, D. G., E. D. Heron, and C. A. Nieduszynski, 2018 Rapid high-resolution measurement of DNA replication timing by droplet digital PCR. *Nucleic Acids Res.* 46: e112. <https://doi.org/10.1093/nar/gky590>
- Berger, C. M., X. Gaume, and P. Bouvet, 2015 The roles of nucleolin subcellular localization in cancer. *Biochimie* 113: 78–85. <https://doi.org/10.1016/j.biochi.2015.03.023>
- Bhattacharjee, A., Y. Wang, J. Diao, and C. M. Price, 2017 Dynamic DNA binding, junction recognition and G4 melting activity underlie the telomeric and genome-wide roles of human CST. *Nucleic Acids Res.* 45: 12311–12324. <https://doi.org/10.1093/nar/gkx878>
- Bochman, M. L., K. Paeschke, and V. A. Zakian, 2012 DNA secondary structures: stability and function of G-quadruplex structures. *Nat. Rev. Genet.* 13: 770–780. <https://doi.org/10.1038/nrg3296>
- Brázda, V., L. Haronikova, J. C. Liao, and M. Fojta, 2014 DNA and RNA quadruplex-binding proteins. *Int. J. Mol. Sci.* 15: 17493–17517. <https://doi.org/10.3390/ijms151017493>
- Cantor, S. B., D. W. Bell, S. Ganesan, E. M. Kass, R. Drapkin *et al.*, 2001 BACH1, a novel helicase-like protein, interacts directly with BRCA1 and contributes to its DNA repair function. *Cell* 105: 149–160. [https://doi.org/10.1016/S0092-8674\(01\)00304-X](https://doi.org/10.1016/S0092-8674(01)00304-X)
- Capra, J. A., K. Paeschke, M. Singh, and V. A. Zakian, 2010 G-quadruplex DNA sequences are evolutionarily conserved and associated with distinct genomic features in *Saccharomyces cerevisiae*. *PLOS Comput. Biol.* 6: e1000861. <https://doi.org/10.1371/journal.pcbi.1000861>
- Chen, C., and R. D. Kolodner, 1999 Gross chromosomal rearrangements in *Saccharomyces cerevisiae* replication and recombination defective mutants. *Nat. Genet.* 23: 81–85. <https://doi.org/10.1038/12687>
- Cogoi, S., A. E. Shchekotikhin, and L. E. Xodo, 2014 HRAS is silenced by two neighboring G-quadruplexes and activated by MAZ, a zinc-finger transcription factor with DNA unfolding property. *Nucleic Acids Res.* 42: 8379–8388. <https://doi.org/10.1093/nar/gku574>
- Dempsey, L. A., H. Sun, L. A. Hanakahi, and N. Maizels, 1999 G4 DNA binding by LR1 and its subunits, nucleolin and hnRNP D, A role for G-G pairing in immunoglobulin switch recombination. *J. Biol. Chem.* 274: 1066–1071. <https://doi.org/10.1074/jbc.274.2.1066>
- Du, Z., Y. Zhao, and N. Li, 2008 Genome-wide analysis reveals regulatory role of G4 DNA in gene transcription. *Genome Res.* 18: 233–241. <https://doi.org/10.1101/gr.6905408>
- Eddy, J., and N. Maizels, 2008 Conserved elements with potential to form polymorphic G-quadruplex structures in the first intron of human genes. *Nucleic Acids Res.* 36: 1321–1333. <https://doi.org/10.1093/nar/gkm1138>
- Erard, M. S., P. Belenguer, M. Caizergues-Ferrer, A. Pantaloni, and F. Amalric, 1988 A major nucleolar protein, nucleolin, induces chromatin decondensation by binding to histone H1. *Eur. J. Biochem.* 175: 525–530. <https://doi.org/10.1111/j.1432-1033.1988.tb14224.x>
- Fry, M., 2007 Tetraplex DNA and its interacting proteins. *Front. Biosci.* 12: 4336–4351. <https://doi.org/10.2741/2391>
- Gallo, A., C. Lo Sterzo, M. Mori, A. Di Matteo, I. Bertini *et al.*, 2012 Structure of nucleophosmin DNA-binding domain and analysis of its complex with a G-quadruplex sequence from the c-MYC promoter. *J. Biol. Chem.* 287: 26539–26548. <https://doi.org/10.1074/jbc.M112.371013>
- Ghosh, M., and M. Singh, 2018 RGG-box in hnRNP A1 specifically recognizes the telomere G-quadruplex DNA and enhances the G-quadruplex unfolding ability of UP1 domain. *Nucleic Acids Res.* 46: 10246–10261. <https://doi.org/10.1093/nar/gky854>
- González, V., and L. H. Hurley, 2010 The C-terminus of nucleolin promotes the formation of the c-MYC G-quadruplex and inhibits c-MYC promoter activity. *Biochemistry* 49: 9706–9714. <https://doi.org/10.1021/bi100509s>
- González, V., K. Guo, L. Hurley, and D. Sun, 2009 Identification and characterization of nucleolin as a c-myc G-quadruplex-binding protein. *J. Biol. Chem.* 284: 23622–23635. <https://doi.org/10.1074/jbc.M109.018028>
- Haeusler, A. R., C. J. Donnelly, G. Periz, E. A. Simko, P. G. Shaw *et al.*, 2014 C9orf72 nucleotide repeat structures initiate molecular cascades of disease. *Nature* 507: 195–200. <https://doi.org/10.1038/nature13124>
- Hanakahi, L. A., H. Sun, and N. Maizels, 1999 High affinity interactions of nucleolin with G-G-paired rDNA. *J. Biol. Chem.* 274: 15908–15912. <https://doi.org/10.1074/jbc.274.22.15908>
- Hanakahi, L. A., Z. Bu, and N. Maizels, 2000 The C-terminal domain of nucleolin accelerates nucleic acid annealing. *Biochemistry* 39: 15493–15499. <https://doi.org/10.1021/bi001683y>
- Han, J., and A. van Hoof, 2016 The RNA exosome channeling and direct access conformations have distinct *in vivo* functions. *Cell Rep.* 16: 3348–3358. <https://doi.org/10.1016/j.celrep.2016.08.059>
- Hershman, S. G., Q. Chen, J. Y. Lee, M. L. Kozak, P. Yue *et al.*, 2008 Genomic distribution and functional analyses of potential G-quadruplex-forming sequences in *Saccharomyces cerevisiae*. *Nucleic Acids Res.* 36: 144–156. <https://doi.org/10.1093/nar/gkm986>
- Huber, M. D., D. C. Lee, and N. Maizels, 2002 G4 DNA unwinding by BLM and Sgs1p: substrate specificity and substrate-specific inhibition. *Nucleic Acids Res.* 30: 3954–3961. <https://doi.org/10.1093/nar/gkf530>
- Huppert, J. L., and S. Balasubramanian, 2005 Prevalence of quadruplexes in the human genome. *Nucleic Acids Res.* 33: 2908–2916. <https://doi.org/10.1093/nar/gki609>
- Indig, F. E., I. Rybanska, P. Karmakar, C. Devulapalli, H. Fu *et al.*, 2012 Nucleolin inhibits G4 oligonucleotide unwinding by



- Werner helicase. *PLoS One* 7: e35229. <https://doi.org/10.1371/journal.pone.0035229>
- Ivessa, A. S., B. A. Lenzmeier, J. B. Bessler, L. K. Goudsouzian, S. L. Schnakenberg *et al.*, 2003 The *Saccharomyces cerevisiae* helicase Rrm3p facilitates replication past nonhistone protein-DNA complexes. *Mol. Cell* 12: 1525–1536. [https://doi.org/10.1016/S1097-2765\(03\)00456-8](https://doi.org/10.1016/S1097-2765(03)00456-8)
- Kim, N., 2019 The interplay between G-quadruplex and transcription. *Curr. Med. Chem.* 26: 2898–2917. <https://doi.org/10.2174/0929867325666171229132619>
- Kim, N., and S. Jinks-Robertson, 2011 Guanine repeat-containing sequences confer transcription-dependent instability in an orientation-specific manner in yeast. *DNA Repair (Amst.)* 10: 953–960. <https://doi.org/10.1016/j.dnarep.2011.07.002>
- Kim, N., A. L. Abdulovic, R. Gealy, M. J. Lippert, and S. Jinks-Robertson, 2007 Transcription-associated mutagenesis in yeast is directly proportional to the level of gene expression and influenced by the direction of DNA replication. *DNA Repair (Amst.)* 6: 1285–1296. <https://doi.org/10.1016/j.dnarep.2007.02.023>
- Kondo, K., and M. Inouye, 1992 Yeast NSR1 protein that has structural similarity to mammalian nucleolin is involved in pre-rRNA processing. *J. Biol. Chem.* 267: 16252–16258.
- Lee, W. C., Z. X. Xue, and T. Melese, 1991 The NSR1 gene encodes a protein that specifically binds nuclear localization sequences and has two RNA recognition motifs. *J. Cell Biol.* 113: 1–12. <https://doi.org/10.1083/jcb.113.1.1>
- Lee, W. C., D. Zabetakis, and T. Melese, 1992 NSR1 is required for pre-rRNA processing and for the proper maintenance of steady-state levels of ribosomal subunits. *Mol. Cell. Biol.* 12: 3865–3871. <https://doi.org/10.1128/MCB.12.9.3865>
- Li, Q. J., X. J. Tong, Y. M. Duan, and J. Q. Zhou, 2013 Characterization of the intramolecular G-quadruplex promoting activity of Est1. *FEBS Lett.* 587: 659–665. <https://doi.org/10.1016/j.febslet.2013.01.024>
- Lopes, J., A. Piazza, R. Bermejo, B. Kriegsman, A. Colosio *et al.*, 2011 G-quadruplex-induced instability during leading-strand replication. *EMBO J.* 30: 4033–4046. <https://doi.org/10.1038/emboj.2011.316>
- Lopez, C. R., S. Singh, S. Hambarde, W. C. Griffin, J. Gao *et al.*, 2017 Yeast Sub1 and human PC4 are G-quadruplex binding proteins that suppress genome instability at co-transcriptionally formed G4 DNA. *Nucleic Acids Res.* 45: 5850–5862. <https://doi.org/10.1093/nar/gkx201>
- Maizels, N., 2015 G4-associated human diseases. *EMBO Rep.* 16: 910–922. <https://doi.org/10.15252/embr.201540607>
- Maizels, N., and L. T. Gray, 2013 The G4 genome. *PLoS Genet.* 9: e1003468. <https://doi.org/10.1371/journal.pgen.1003468>
- Majounie, E., Y. Abramzon, A. E. Renton, R. Perry, S. S. Bassett *et al.*, 2012 Repeat expansion in C9ORF72 in Alzheimer's disease. *N. Engl. J. Med.* 366: 283–284. <https://doi.org/10.1056/NEJMc1113592>
- Megonigal, M. D., J. Fertala, and M. A. Bjornsti, 1997 Alterations in the catalytic activity of yeast DNA topoisomerase I result in cell cycle arrest and cell death. *J. Biol. Chem.* 272: 12801–12808. <https://doi.org/10.1074/jbc.272.19.12801>
- Mendoza, O., A. Bourdoncle, J. B. Boule, R. M. Brosh, Jr., and J. L. Mergny, 2016 G-quadruplexes and helicases. *Nucleic Acids Res.* 44: 1989–2006. <https://doi.org/10.1093/nar/gkw079>
- Moruno-Manchon, J. F., E. C. Koellhoffer, J. Gopakumar, S. Hambarde, N. Kim *et al.*, 2017 The G-quadruplex DNA stabilizing drug pyridostatin promotes DNA damage and downregulates transcription of *Brc1* in neurons. *Aging (Albany NY)* 9: 1957–1970. <https://doi.org/10.18632/aging.101282>
- Otake, Y., S. Soundararajan, T. K. Sengupta, E. A. Kio, J. C. Smith *et al.*, 2007 Overexpression of nucleolin in chronic lymphocytic leukemia cells induces stabilization of *bcl2* mRNA. *Blood* 109: 3069–3075. <https://doi.org/10.1182/blood-2006-08-043257>
- Owiti, N., S. Wei, A. S. Bhagwat, and N. Kim, 2018 Unscheduled DNA synthesis leads to elevated uracil residues at highly transcribed genomic loci in *Saccharomyces cerevisiae*. *PLoS Genet.* 14: e1007516. <https://doi.org/10.1371/journal.pgen.1007516>
- Paeschke, K., M. L. Bochman, P. D. Garcia, P. Cejka, K. L. Friedman *et al.*, 2013 Pif1 family helicases suppress genome instability at G-quadruplex motifs. *Nature* 497: 458–462. <https://doi.org/10.1038/nature12149>
- Pedroso, I. M., W. Hayward, and T. M. Fletcher, 2009 The effect of the TRF2 N-terminal and TRFH regions on telomeric G-quadruplex structures. *Nucleic Acids Res.* 37: 1541–1554. <https://doi.org/10.1093/nar/gkn1081>
- Peled, J. U., F. L. Kuang, M. D. Iglesias-Ussel, S. Roa, S. L. Kalis *et al.*, 2008 The biochemistry of somatic hypermutation. *Annu. Rev. Immunol.* 26: 481–511. <https://doi.org/10.1146/annurev.immunol.26.021607.090236>
- Piazza, A., A. Serero, J. B. Boule, P. Legoix-Ne, J. Lopes *et al.*, 2012 Stimulation of gross chromosomal rearrangements by the human CEB1 and CEB25 minisatellites in *Saccharomyces cerevisiae* depends on G-quadruplexes or Cdc13. *PLoS Genet.* 8: e1003033. <https://doi.org/10.1371/journal.pgen.1003033>
- Pinheiro, L. B., V. A. Coleman, C. M. Hindson, J. Herrmann, B. J. Hindson *et al.*, 2012 Evaluation of a droplet digital polymerase chain reaction format for DNA copy number quantification. *Anal. Chem.* 84: 1003–1011. <https://doi.org/10.1021/ac202578x>
- Rawal, P., V. B. Kummarasetti, J. Ravindran, N. Kumar, K. Halder *et al.*, 2006 Genome-wide prediction of G4 DNA as regulatory motifs: role in *Escherichia coli* global regulation. *Genome Res.* 16: 644–655. <https://doi.org/10.1101/gr.4508806>
- Sarkies, P., C. Reams, L. J. Simpson, and J. E. Sale, 2010 Epigenetic instability due to defective replication of structured DNA. *Mol. Cell* 40: 703–713. <https://doi.org/10.1016/j.molcel.2010.11.009>
- Satake, Y., Y. Kuwano, T. Nishikawa, K. Fujita, S. Saijo *et al.*, 2018 Nucleolin facilitates nuclear retention of an ultraconserved region containing TRA2beta4 and accelerates colon cancer cell growth. *Oncotarget* 9: 26817–26833. <https://doi.org/10.18632/oncotarget.25510>
- Seal, S., D. Thompson, A. Renwick, A. Elliott, P. Kelly *et al.*, 2006 Truncating mutations in the Fanconi anemia J gene BRIP1 are low-penetrance breast cancer susceptibility alleles. *Nat. Genet.* 38: 1239–1241. <https://doi.org/10.1038/ng1902>
- Seenisamy, J., E. M. Rezler, T. J. Powell, D. Tye, V. Gokhale *et al.*, 2004 The dynamic character of the G-quadruplex element in the c-MYC promoter and modification by TMPyP4. *J. Am. Chem. Soc.* 126: 8702–8709. <https://doi.org/10.1021/ja040022b>
- Siddiqui-Jain, A., C. L. Grand, D. J. Bearss, and L. H. Hurley, 2002 Direct evidence for a G-quadruplex in a promoter region and its targeting with a small molecule to repress c-MYC transcription. *Proc. Natl. Acad. Sci. USA* 99: 11593–11598. <https://doi.org/10.1073/pnas.182256799>
- Spell, R. M., and S. Jinks-Robertson, 2004 Determination of mitotic recombination rates by fluctuation analysis in *Saccharomyces cerevisiae*. *Methods Mol. Biol.* 262: 3–12. <https://doi.org/10.1385/1-59259-761-0:003>
- Sun, H., J. K. Karow, I. D. Hickson, and N. Maizels, 1998 The Bloom's syndrome helicase unwinds G4 DNA. *J. Biol. Chem.* 273: 27587–27592. <https://doi.org/10.1074/jbc.273.42.27587>
- Tajrish, M. M., R. Tuteja, and N. Tuteja, 2011 Nucleolin: the most abundant multifunctional phosphoprotein of nucleolus. *Commun. Integr. Biol.* 4: 267–275. <https://doi.org/10.4161/cib.4.3.14884>
- Thandapani, P., T. R. O'Connor, T. L. Bailey, and S. Richard, 2013 Defining the RGG/RG motif. *Mol. Cell* 50: 613–623. <https://doi.org/10.1016/j.molcel.2013.05.021>

- Todd, A. K., M. Johnston, and S. Neidle, 2005 Highly prevalent putative quadruplex sequence motifs in human DNA. *Nucleic Acids Res.* 33: 2901–2907. <https://doi.org/10.1093/nar/gki553>
- Tosoni, E., I. Frasson, M. Scalabrin, R. Perrone, E. Butovskaya *et al.*, 2015 Nucleolin stabilizes G-quadruplex structures folded by the LTR promoter and silences HIV-1 viral transcription. *Nucleic Acids Res.* 43: 8884–8897. <https://doi.org/10.1093/nar/gkv897>
- Wahba, L., J. D. Amon, D. Koshland, and M. Vuica-Ross, 2011 RNase H and multiple RNA biogenesis factors cooperate to prevent RNA:DNA hybrids from generating genome instability. *Mol. Cell* 44: 978–988. <https://doi.org/10.1016/j.molcel.2011.10.017>
- Williams, J. D., S. Fleetwood, A. Berroyer, N. Kim, and E. D. Larson, 2015 Sites of instability in the human TCF3 (E2A) gene adopt G-quadruplex DNA structures in vitro. *Front. Genet.* 6: 177. <https://doi.org/10.3389/fgene.2015.00177>
- Williams, J. D., D. Houserova, B. R. Johnson, B. Dyniewski, A. Berroyer *et al.*, 2020 Characterization of long G4-rich enhancer-associated genomic regions engaging in a novel loop-loop 'G4 Kissing' interaction. *Nucleic Acids Res.* 48: 5907–5925. <https://doi.org/10.1093/nar/gkaa357>
- Wu, Y., K. Shin-ya, and R. M. Brosh, Jr., 2008 FANCD1 helicase defective in Fanconi anemia and breast cancer unwinds G-quadruplex DNA to defend genomic stability. *Mol. Cell Biol.* 28: 4116–4128. <https://doi.org/10.1128/MCB.02210-07>
- Yadav, P., V. Harcy, J. L. Argueso, M. Dominska, S. Jinks-Robertson *et al.*, 2014 Topoisomerase I plays a critical role in suppressing genome instability at a highly transcribed G-quadruplex-forming sequence. *PLoS Genet.* 10: e1004839. <https://doi.org/10.1371/journal.pgen.1004839>
- Yadav, P., N. Owiti, and N. Kim, 2016 The role of topoisomerase I in suppressing genome instability associated with a highly transcribed guanine-rich sequence is not restricted to preventing RNA:DNA hybrid accumulation. *Nucleic Acids Res.* 44: 718–729. <https://doi.org/10.1093/nar/gkv1152>

*Communicating editor: D. Bishop*